RSC Advances

ROYAL SOCIETY OF CHEMISTRY

www.rsc.org/advances

Electrochemical synthesis of ammonia from wet nitrogen using $La_{0.6}Sr_{0.4}FeO_{3-\delta}$ - $Ce_{0.8}Gd_{0.18}Ca_{0.02}O_{2-\delta}$ composite cathode

Ibrahim A. Amar, Christophe T.G. Petit, Rong Lan, Gregory Mann and Shanwen Tao*

Department of Chemical & Process Engineering, University of Strathclyde, Glasgow G1 1XJ, UK

ABSTRACT

Electrochemical synthesis of ammonia from wet nitrogen in an electrolytic cell using a $La_{0.6}Sr_{0.4}FeO_{3-\delta}$ - $Ce_{0.8}Gd_{0.18}Ca_{0.02}O_{2-\delta}$ composite cathode and an oxide-carbonate composite electrolyte has been investigated. $La_{0.6}Sr_{0.4}FeO_{3-\delta}$ was prepared via a combined EDTA-citrate complexing sol-gel process, characterised by X-ray diffraction and SEM. A tri-layer electrolytic cell was fabricated by a one-step dry-pressing and co-firing process. Ammonia was successfully synthesised from wet nitrogen under atmospheric pressure. Ammonia formation was observed at 375, 400, 425 and 450 ºC and the maximum ammonia formation rate of 7×10^{-11} mol s^{-1} cm^{-2} was observed at 400 ºC when a voltage of 1.4 V was applied. This ammonia formation rate corresponds to Faradaic efficiency of ~ 0.14 % at current density of 14.25 mA/cm^2.

Keywords: electrochemical synthesis of ammonia; water; nitrogen; perovskite oxide; oxide-carbonate composite electrolyte

* Corresponding author:

Department of Chemical and Process Engineering,

University of Strathclyde, Glasgow G1 1XJ, UK

Tel. +44 (0) 141 548 2361; Fax: +44 (0) 141 548 2539
E-mail: shanwen.tao@strath.ac.uk

1. Introduction

Ammonia is an important chemical and the second most produced chemicals worldwide. In 2011, the global production of ammonia was 136 million metric tons.[1, 2] In addition, approximately 80 % of the globally produced ammonia are consumed in fertiliser industry and the rest are used in other industries including plastics, refrigeration, transportation, pharmaceuticals and explosives production.[3-6] The Haber-Bosch process, invented in 1904, is still the dominant route for ammonia production on a large scale. This process involves the reaction of gaseous hydrogen and nitrogen on Fe-based catalyst at high temperature (~ 500 °C) and high pressure (150-300 bar). In this process, the required H_2 for ammonia synthesis is produced entirely through the steam reforming of natural gases or coal. In addition, approximately 84 % of the energy required for the ammonia industry is consumed in the steam reforming step. Moreover, 2.3 tons CO_2 are released when a ton of ammonia is produced,[1, 7, 8] This means that alternative energy sources is of crucial importance for reducing CO_2 emission from ammonia industry. Electrochemical syntheses of ammonia is among the promising alternatives to the Haber Bosch process.[9-12] In these processes, cells based on different electrolyte materials have been investigated, including liquids,[13-15] molten salts[16, 17] and solid state ionic conductors.[18-23]

Perovskite oxides have attracted considerable interest due to their ease of synthesis, high thermal stability, good catalytic activity and low cost.[24] These oxides have been widely used as electrocatalysts in many applications, including solid oxide fuel cells (SOFCs) [25, 26] and solid oxide steam electrolysis cells (SOECs).[27, 28] In terms of electrochemical synthesis of ammonia, perovskite-based oxides such as $Sm_{0.5}Sr_{0.5}CoO_{3-\delta}$ (SSCo) and $SmFe_{0.7}Cu_{0.1}Ni_{0.2}O_{3-\delta}$ (SFCN) have been used as cathode materials for synthesis of ammonia from its elements (H_2 and N_2) at low temperature (25-100 °C).[29, 30] In addition, the electrocatalytic activity of these oxides for ammonia synthesis has also been studied at intermediate temperature (400-600 °C). Recently, ammonia was successfully synthesised from H_2 and N_2 in an electrolytic cell using $Ba_{0.5}Sr_{0.5}Co_{0.8}Fe_{0.2}O_{3-\delta}$, (BSCF) and $La_{0.6}Sr_{0.4}Fe_{0.8}Cu_{0.2}O_{3-\delta}$, (LSFCu) as cathodes. [21, 31] Here we report the electrochemical synthesis of ammonia from H_2O and N_2 in

electrolytic cell using $La_{0.6}Sr_{0.4}FeO_{3-\delta}$- $Ce_{0.8}Gd_{0.18}Ca_{0.02}O_{2-\delta}$ (LSF-CGDC) composite as a cathode and, doped ceria-carbonate composite as an oxygen-ion (O^{2-}) conducing electrolyte.

2. Experimental

2.1 Materials synthesis

$La_{0.6}Sr_{0.4}FeO_{3-\delta}$ (LSF) catalyst was synthesised via a combined EDTA-citrate complexing sol-gel process.[32] Lanthanum oxide (La_2O_3, Alfa Aesar, 99 %), strontium nitrate ($Sr(NO_3)_2$, Alfa Aesar, 99 %) and iron nitrate nanohydrate ($Fe(NO_3)_3 \cdot 9H_2O$, Alfa Aesar, 98 %) were used as starting materials. 2.1993g La_2O_3 was dissolved in diluted nitric acid to form lanthanum nitrate. 1.9047g $Sr(NO_3)_2$ and 9.0898g $Fe(NO_3)_3 \cdot 9H_2O$ were dissolved in deionised water and then added to the lanthanum nitrate solution. 12.9681g Citric acid and 13.1508g EDTA were then added as complexing agents, with molar ratio of citric acid:EDTA:metal cations of 1.5:1:1. $NH_3 \cdot H_2O$ was added to the mixed solution to adjust the pH value to around 6. Under heating and stirring, the solution was evaporated on a hot-plate, and then gradually changed into a black sticky gel before complete drying. The resultant powder was ground and subsequently fired in a muffle furnace (Carbolite) in air at 900 ºC for 2 h with a heating/cooling rate of 5 ºC min^{-1} to obtain a pure phase of LSF catalyst.

$Sm_{0.5}Sr_{0.5}CoO_{3-\delta}$ (SSCo) catalyst and Gd and Ca co-doped ceria $Ce_{0.8}Gd_{0.18}Ca_{0.02}O_{2-\delta}$ (CGDC) powders were also synthesised via a combined EDTA-citrate complexing sol-gel process as described elsewhere. The composite electrolyte CGDC-$(Li/Na/K)_2CO_3$ (70:30 wt%) was prepared as described elsewhere.[23]

2.2 Materials Characterisation

X-ray diffraction (XRD) data were collected at room temperature using a Panalytical X'Pert Pro diffractometer with Ni-filtered CuKα radiation (λ=1.5405 Å), using 40 kV and 40 mA, fitted with a X'Celerator detector. Absolute scans were recorded in the 2θ range 5-100º, with a step size of 0.0167º.

The microstructures of the prepared catalyst and the cross-sectional area of the single cell were examined using a Hitachi SU6600 Scanning Electron Microscope (SEM).

Thermogravimetry and differential scanning calorimetry (TGA/DSC) analyses were performed using a Stanton Redcroft STA/TGH series STA 1500, operating through a Rheometric Scientific system interface controlled by the software RSI Orchestrator. The thermal behaviour of the perovskite based cathode (LSF) was investigated in N_2 atmosphere from room temperature to 500 ºC with a heating/cooling rate of 10 ºC/min.

2.3 Fabrication of the single cell for ammonia synthesis

A tri-layer single cell was fabricated by a cost-effective, one-step, dry-pressing method. The composite anode was prepared by mixing SSCo, CGDC and a pore former (starch) in a mortar with weight ratio of 70:30:15. The composite electrolyte consists of CGDC/$(Li/Na/K)_2CO_3$ (70:30 wt %). The composite cathode was prepared by mixing in a mortar LSF and CGDC and starch, with weight ratio of 70:30:15. The composite anode, electrolyte and cathode were fed into the die, layer by layer, with the aid of a sieve to ensure uniform powder distribution, and then uniaxially pressed under a pressure of 121 MPa. This freshly made green pellet was sintered in air at 700 °C for 2 h, at a heating/cooling rate of 2°C/min. The active surface area of the cathode was 0.785 cm^2. Silver paste was painted in a grid pattern on each electrode surface of the cell, as a current collector. Ag wires were used as output terminals for both electrodes.

2.5 Ammonia synthesis

The fabricated single cells for ammonia synthesis were sealed into a self-designed double-chamber reactor, using ceramic sealant. The electrolytic cell for ammonia was constructed as follows: Air, SSCo-CGDC|CGDC-carbonate|LSF-CGDC, 3% H_2O-N_2. The cathode chamber was fed with 3% H_2O-N_2. N2 was bubbling through room temperature water before feeding into the cathode chamber. The anode was exposed to air. The voltage was applied by a Solartron 1287A electrochemical interface controlled by software CorrWare/CorrView for automatic data collection. A constant voltage was applied to the cell for 30 min. The synthesised ammonia at the cathode chamber was absorbed by 20 ml of diluted hydrochloric acid (0.01 M). The concentration of NH_4^+ in the absorbed solution was analysed using ISE (Thermo Scientific Orion Star A214). The rate of ammonia formation was calculated using **Error! Reference source not found.**:

$$r_{NH_3} = \frac{[NH_4^+] \times V}{t \times A} \quad (1)$$

where $[NH_4^+]$ is the measured NH_4^+ ion concentration, V is the volume of the diluted hydrochloric acid used for ammonia collection, t is the absorption time and A is the effective area of the catalyst.

AC impedance spectroscopy (IS) measurements were performed using a Schlumberger Solarton SI 1250 analyser, coupled with a SI 1287A Electrochemical Interface controlled by Z-plot/Z-view software. The AC impedance spectra were recorded over the frequency range 65 kHz to 0.01 Hz.

3. Results and discussion

3.1 XRD and SEM

Single-phase perovskite oxide $La_{0.6}Sr_{0.4}FeO_{3-\delta}$ (LSF) was obtained when the corresponding ash was calcined in air at 900 °C for 2 h. The X-ray diffraction pattern of LSF (Fig. 1a) shows a typical cubic perovskite oxide structure, which is in good agreement with JCPDS file 39-1083. The crystallite size of LSF is about 31.58 nm, estimated from Sherrer's formula. Fig. 1c shows the XRD pattern of LSF-CGDC composite cathode (70:30 wt %) fired in air at 700 °C, the sintering temperature of the single cell for ammonia synthesis. The composite cathode displays only the characteristic peaks of pure LSF (Fig. 1a) and pure CGDC (Fig. 1b). This indicates that LSF is chemically compatible with CGDC at the single cell sintering temperature.

The microstructure of LSF powder calcined in air at 900 °C for 2 h was examined by scanning electron microscopy (SEM) (Fig. 2a). The SEM image of LSF oxide shows microporous structure with fine agglomerated particles of different sizes and shapes. The SEM micrograph of the cross-section view of the single cell (before test) sintered in air at 700 ºC for 2 h is shown in Fig. 2b. The CGDC-carbonate composite electrolyte is dense with good cathode/electrolyte and anode/electrolyte interfaces. This indicates that the composite electrolyte is thermally compatible with both composite electrodes.

3.2 Thermal analysis

Fig. 3 shows the TGA-DSC curves of the LSF cathode in N_2, from room temperature to 500 °C, at heating/cooling rate of 10 °C/min. Between room temperature and 200 ºC, a weight loss of about 0.67 wt% was observed, which could be attributed to the loss of adsorbed water. A slight weight loss of about 0.25 wt % was observed between 200 and 500 ºC, , , which could be due to the loss of lattice oxygen from the $La_{0.6}Sr_{0.4}FeO_{3-\delta}$.

Fig. 4a & b show the XRD patterns of the perovskite-based cathode (LSF) before and after thermal analysis in N_2 atmosphere respectively. The oxide retained the same perovskite structure and no extra peaks were observed, indicating the thermal stability of LSF cathode under N_2 atmosphere in the measured temperature range.

3.3 Synthesis of ammonia at different temperatures

Fig. 5 represents the performance stability of the electrolytic cell during the synthesis of ammonia at different temperatures (375-450 °C), with an applied voltage of 1.4 V, over a period of 30 min. The electrolytic cell demonstrated stable performance at the operating temperatures. Furthermore, the generated current densities increased as the operating temperature increased and reached a maximum value of 28.54 mA/cm^2 at 450 °C. This increases in current density with increased operating temperature is attributed to the enhancement in the ionic conductivity of the electrolyte at high temperature and decrease in electrode polarisation resistance.

Fig. 6 shows the in-situ AC impedance spectra under open circuit conditions at different temperatures (375-450 °C). The series resistance, which is mainly related to the ohmic resistance of the electrolyte and the electrolyte/electrode interfaces, decreased significantly with an increase the in cell operating temperature, and the lowest value of 4.17 Ω cm^2, was attained at 450 °C. This decrease in the ohmic resistance with temperature could be due to the increase in the ionic conductivity of the composite electrolyte with temperature. In addition, the total polarisation resistance also decreased significantly when the operating temperature was increased, which could be due to the improvement in the catalytic activity of the composite cathode (LSF-CGDC) with increased temperature.

The relationship between the ammonia formation rate and the operating temperature was investigated under a constant voltage of 1.4 V (Fig. 7). The ammonia formation rate increased with increased operating temperature. The maximum value was attained when the electrolytic cell operated at 400 ºC. Moreover, the maximum ammonia formation rate of 7.0 $\times 10^{-11}$ mol s^{-1} cm^{-2} was observed at 400 °C. The current density was 14.25 mA/cm^2 and the corresponding Faradaic efficiency was 0.14 %. In addition, the increase in ammonia formation rate with an increase in operating temperature from 375 to 400 °C could be attributed to the increase in the ionic conductivity of the electrolyte with temperature.[21, 33] However, when the electrolytic cells operated at a temperature above 400 ºC, the ammonia formation rate decreased. This decrease in the rate at high temperature might be due to the thermal decomposition of ammonia,[34] although the electrolyte ionic conductivity increases with temperature.[21, 31]

3.4 Synthesis of ammonia at different applied voltages

Fig. 8 shows the current density across the cell at 400 °C when applied a voltage between 1.2-1.8 V over a period of 30 minutes. The initial current drop could be related to the ion 'blocking effect' which was also observed in previous reports in cells based on oxide-carbonate composite electrolytes.[18, 35, 36] It should be noted that, after the initial stabilisation process, the cell demonstrated almost stable performance under the applied voltages, indicating a stable electrochemical process. In addition, the generated current density increased when the applied voltage increased from 1.2 to 1.4 V, which means that more oxide ions (O^{2-}) were transported through the electrolyte to the anode surface. However, when the applied voltage was further increased, to values higher than 1.4 V, a slight decrease in current density was observed. The ion blocking effect is expected to be more significant at higher voltage which may cause the reduced current. This could be due to the blocking effect of cations such as Li^+, Na^+ and K^+ ions at the electrolyte/cathode interface and the anions such as HCO_3^-, CO_3^{2-} ions at the anode/electrolyte interface. These charged ions may accumulate and form charged layers at the electrolyte/electrode interfaces, partially blocking the transfer of oxygen ions (O^{2-}), resulting in low current densities.[18, 35, 36]

In order to investigate the effects of the applied voltage on the ammonia formation rate, the operating temperature of the electrolytic cell was kept at 400 °C and the applied voltage was varied from 1.2 to 1.8 V (Fig. 9). There is an increase in the ammonia formation rate as the

applied voltage increased from 1.2 to 1.4 V. The ammonia production rate was found to be 7.0×10^{-11} mol s^{-1} cm^{-2} at 400 °C when a voltage of 1.4 V was applied. However, the ammonia formation rate decreased significantly when the applied voltage was further increased and reached the minimum values at applied voltage of 1.8 V. This could be attributed to the competitive adsorption of H_2 and N_2 over the cathode surface.[14, 37] This low rate of ammonia formation, with the corresponding Faradaic efficiencies (< 1%), indicate that there is more than one process over the cathode surface and that the competitive hydrogen evolution reaction (HER) is the dominant one. Although the ammonia formation rates were not high, these values are much higher than those reported previously (3.75×10^{-13} mol s^{-1} cm^{-2} at 650 °C), when steam and nitrogen were used to produce ammonia in an electrolytic cell based on an oxide ion (O^{2-}) conducting electrolyte (YSZ).[20] The difference is believed due to the lower operating temperature in this study. It is envisaged that, in terms of ammonia decomposition, an intermediate operating temperature below 400 °C would be a better choice.

4. Conclusion

Perovskite oxide $La_{0.6}Sr_{0.4}FeO_{3-\delta}$ was synthesised via a combined EDTA-citrate complexing sol-gel process. The properties of LSF, including phase composition, microstructure, and thermal behaviour were investigated. It was found that the oxide was thermally stable in N_2 atmosphere within the measured temperature range (~ 25-500 °C). Tri-layer electrolytic cell was successfully fabricated by a one-step dry-pressing and co-firing process. Ammonia was successfully synthesised directly from wet nitrogen using LSF-CGDC composite cathode, CGCD-carbonate composite electrolyte and SSCo-CGDC composite anode. The maximum ammonia formation rate of 7.0×10^{-11} mol s^{-1} cm^{-2} was observed at 400 °C when a voltage of 1.4 V was applied. Although the ammonia formation rate was not high, this value is two orders of magnitudes higher than those previously reported by Skodra et al. ,[20] when ammonia was synthesised from H_2O and N_2 at 650 °C over a Ru-based catalyst.

Acknowledgement

The authors thank EPSRC SuperGen XIV 'Delivery of Sustainable Hydrogen' project (Grant No EP/G01244X/1) for funding. One of the authors (Ibrahim A. Amar) thanks The Libyan Cultural Affairs, London for the financial support of his study in the UK.

References

1. M. Appl, *Ammonia: principles and industrial practice*, Wiley-VCH Weinheim, Germany, 1999.
2. US and G. Survey, *Mineral Commodity Summaries*, Geological Survey, 2012.
3. G. R. Maxwell, in *Synthetic Nitrogen Products*, Springer US, 2005, pp. 15-42.
4. C. Zamfirescu and I. Dincer, *J. Power Sources*, 2008, **185**, 459-465.
5. G. C. Miller, *J. Chem. Edu.*, 1981, **58**, 424.
6. H. J. Bomelburg, *Plant/Operations Progress*, 1982, **1**, 175-180.
7. I. Rafiqul, C. Weber, B. Lehmann and A. Voss, *Energy*, 2005, **30**, 2487-2504.
8. R. Michalsky and P. H. Pfromm, *Solar Energy*, 2011, **85**, 2642-2654.
9. S. Giddey, S. P. S. Badwal and A. Kulkarni, *Inter.J. Hydrogen Energy*, 2013, **38**, 14576-14594.
10. I. A. Amar, R. Lan, C. T. Petit and S. W. Tao, *J. Solid State Electrochem.*, 2011, **15**, 1845-1860.
11. K. Kugler, B. Ohs, M. Scholz and M. Wessling, *Phys. Chem. Chem. Phys.*, 2014, DOI: 10.1039/C1034CP00173G.
12. I. Garagounis, V. Kyriakou, A. Skodra, E. Vasileiou and M. Stoukides, *Frontiers in Energy Research*, 2014, **2**, doi: 10.3389/fenrg.2014.00001.
13. A. Tsuneto, A. Kudo and T. Sakata, *Chem. Lett.*, 1993, **22**, 851-854.
14. A. Sclafani, V. Augugliaro and M. Schiavello, *J. Electrochem. Soc.*, 1983, **130**, 734-736.
15. F. Köleli and D. B. Kayan, *J. Electroanal. Chem.*, 2010, **638**, 119-122.
16. T. Murakami, T. Nishikiori, T. Nohira and Y. Ito, *J. Amer. Chem. Soc.*, 2003, **125**, 334-335.
17. T. Murakami, T. Nohira, T. Goto, Y. H. Ogata and Y. Ito, *Electrochim. Acta*, 2005, **50**, 5423-5426.
18. R. Lan, K. A. Alkhazmi, I. A. Amar and S. W. Tao, *Appl. Catal. B: Environmental*, 2014, **152–153**, 212-217.
19. G. Marnellos and M. Stoukides, *Science*, 1998, **282**, 98-100.
20. A. Skodra and M. Stoukides, *Solid State Ionics*, 2009, **180**, 1332-1336.
21. W. Wang, X. Cao, W. Gao, F. Zhang, H. Wang and G. Ma, *J. Memb. Sci.*, 2010, **360**, 397-403.
22. R. Q. Liu, Y. H. Xie, J. D. Wang, Z. J. Li and B. H. Wang, *Solid State Ionics*, 2006, **177**, 73-76.
23. I. A. Amar, C. T. G. Petit, G. Mann, R. Lan, P. J. Skabara and S. Tao, *Inter. J. Hydrogen Energy*, 2014, DOI:10.1016/j.ijhydene.2013.12.177.
24. G. Pecchi, M. Jiliberto, E. Delgado, L. Cadús and J. Fierro, *J. Chem. Tech. Biotech.*, 2011, **86**, 1067-1073.
25. C. Xia, W. Rauch, F. Chen and M. Liu, *Solid State Ionics*, 2002, **149**, 11-19.
26. Z. Shao and S. M. Haile, *Nature*, 2004, **431**, 170-173.
27. X. Yue and J. T. S. Irvine, *Solid State Ionics*, 2012, **225**, 131-135.
28. Y. Gan, J. Zhang, Y. Li, S. Li, K. Xie and J. T. Irvine, *J. Electrochem. Soc.*, 2012, **159**, F763-F767.
29. J. Wang and R. Liu, *Acta Chim. Sinica*, 2008, **66**, 717-721.
30. G. C. Xu, R. Q. Liu and J. Wang, *Sci. China Ser. B: Chem.*, 2009, **52**, 1171-1175.
31. I. A. Amar, C. T. G. Petit, L. Zhang, R. Lan, P. J. Skabara and S. W. Tao, *Solid State Ionics*, 2011, **201**, 94-100.

32. Y. Ling, J. Yu, B. lin, X. Zhang, L. Zhao and X. Liu, *J. Power Sources*, 2011, **196**, 2631-2634.
33. I. A. Amar, R. Lan, C. T. G. Petit, V. Arrighi and S. W. Tao, *Solid State Ionics*, 2011, **182**, 133-138.
34. R. Lan, J. T. Irvine and S. W. Tao, *Sci. Rep.*, 2013, **3**, 1145.
35. R. Lan and S. W. Tao, *RSC Adv.*, 2013, **3**, 18016-18021.
36. L. Fan, G. Zhang, M. Chen, C. Wang, J. Di and B. Zhu, *Intern. J. Electrochem. Sci.*, 2012, **7**, 8420-8435.
37. V. Kordali, G. Kyriacou and C. Lambrou, *Chem. Comm.*, 2000, 1673-1674.

List of caption

Fig. 1 XRD patterns of (a) LSF calcined in air at 900 ºC; (b) CGDC calcined in air at 700 ºC; (c) LSF-CGDC composite cathode fired in at 700 ºC.

Fig. 2 SEM images: (a) LSF powders calcined in air at 900 ºC; (b) cross-sectional areas of the single cell before ammonia synthesis.

Fig. 3 TGA-DSC curves for LSF based catalyst in nitrogen, up to 500 ºC.

Fig. 4 XDR patterns of: (a) LSF before thermal analysis; (b) LSF after thermal analysis in N_2

Fig. 5 Electrolytic cell performance stability at 1.4 V and 375-450 ºC.

Fig. 6 Impedance spectra under open circuit conditions.

Fig. 7 Dependence of the rate of ammonia formation on the operating temperature.

Fig. 8 The current density across the cell when applied different voltage at 400 ºC.

Fig. 9 Dependence of the rate of ammonia formation on the applied voltage at 400 ºC

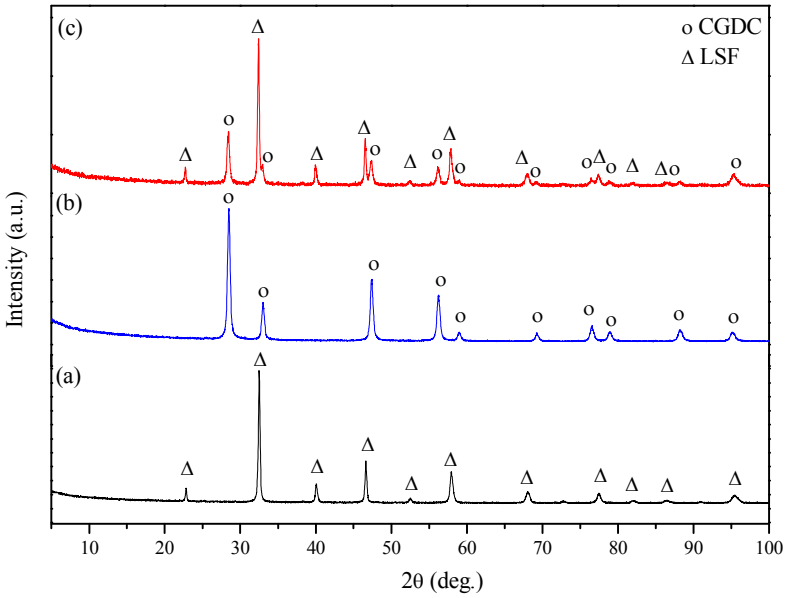

Fig. 1 XRD patterns of (a) LSF calcined in air at 900 ºC; (b) CGDC calcined in air at 700 ºC; (c) LSF-CGDC composite cathode fired in at 700 ºC

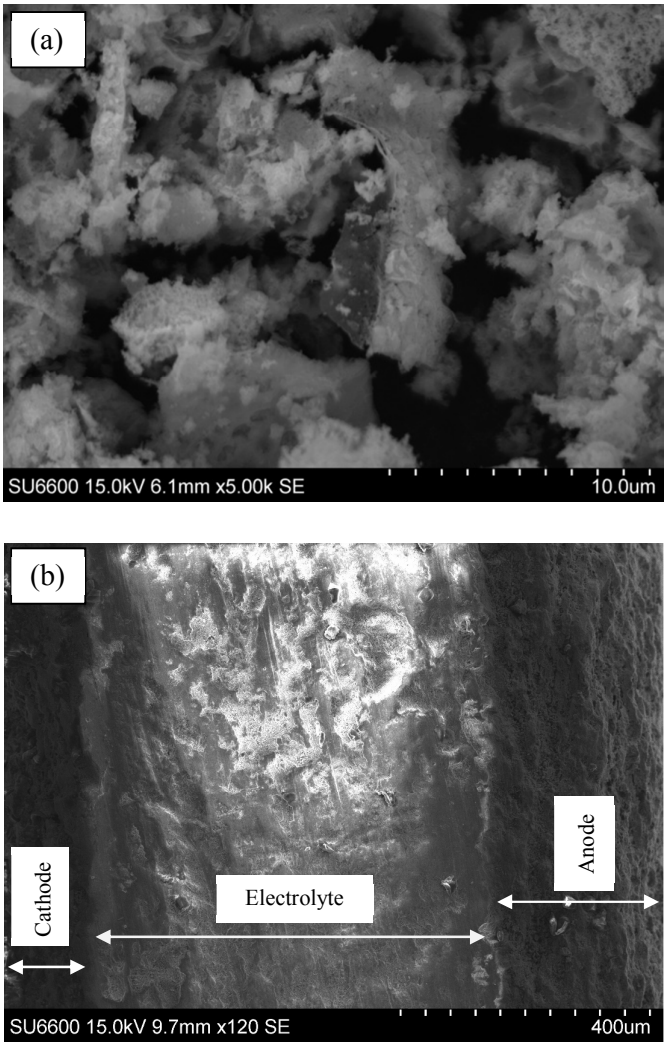

Fig. 2 SEM images: (a) LSF powders calcined in air at 900 ºC; (b) cross-sectional areas of the single cell before ammonia synthesis

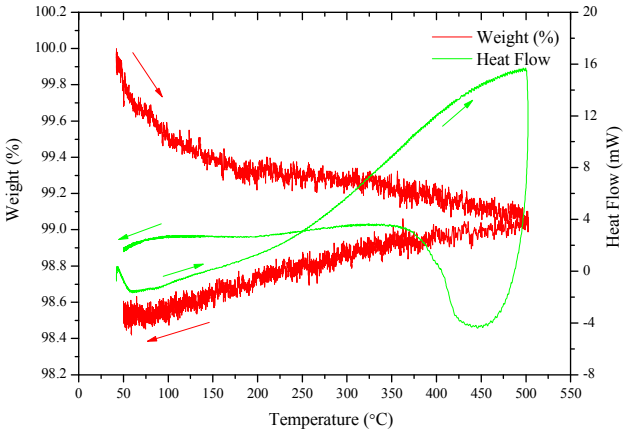

Fig. 3 TGA-DSC curves for LSF based catalyst in nitrogen, up to 500 ºC

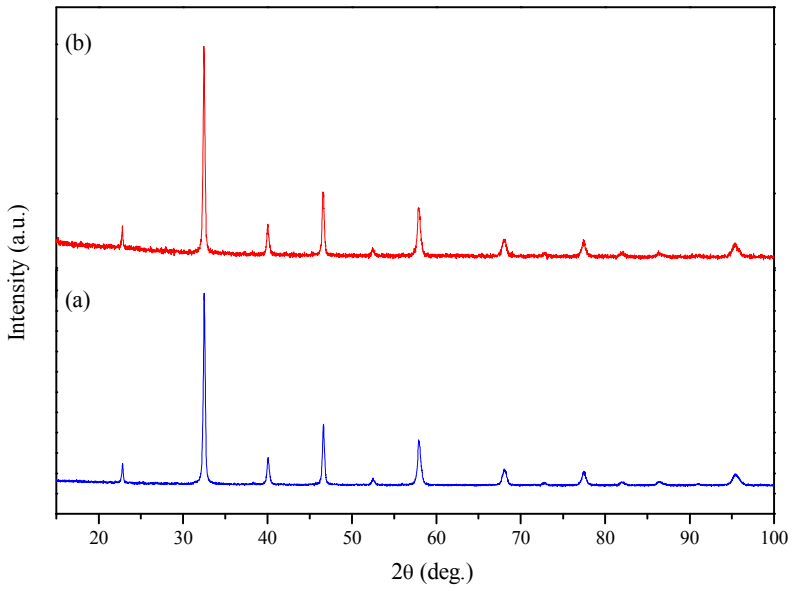

Fig. 4 XDR patterns of: (a) LSF before thermal analysis; (b) LSF after thermal analysis in N_2

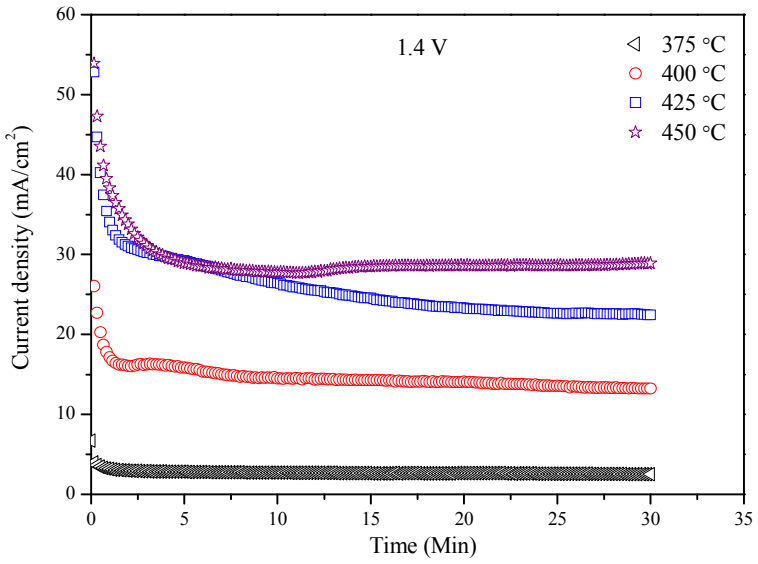

Fig. 5 Electrolytic cell performance stability at 1.4 V and 375-450 °C

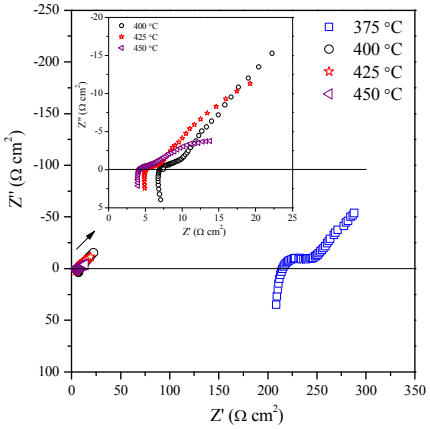

Fig. 6 Impedance spectra under open circuit conditions.

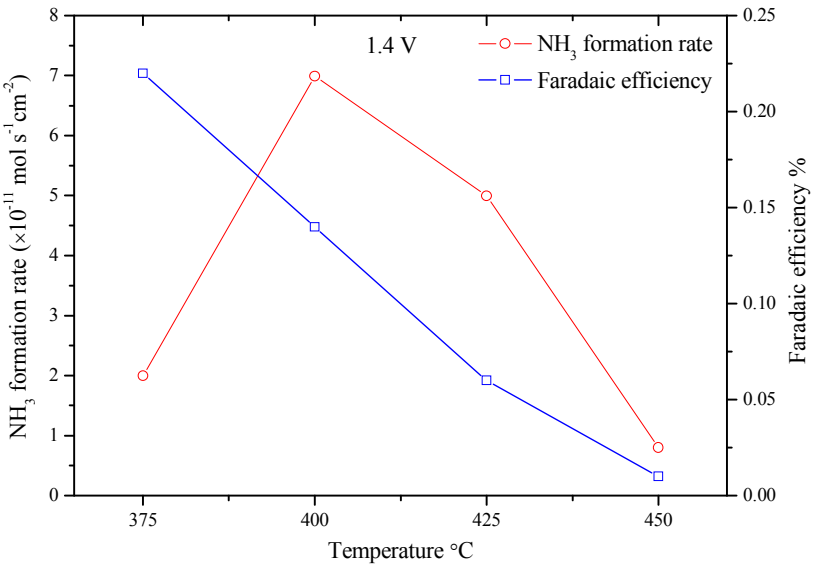

Fig. 7 Dependence of the rate of ammonia formation on the operating temperature

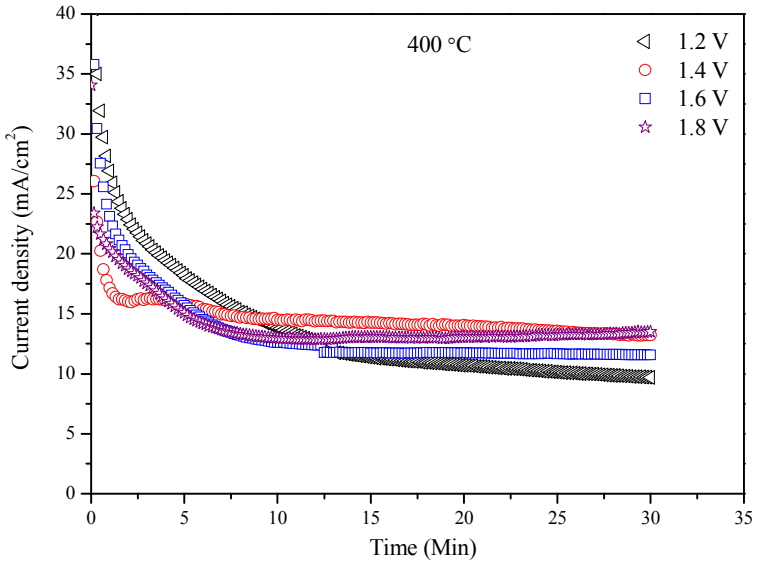

Fig. 8 The current density across the cell when applied different voltage at 400 °C.

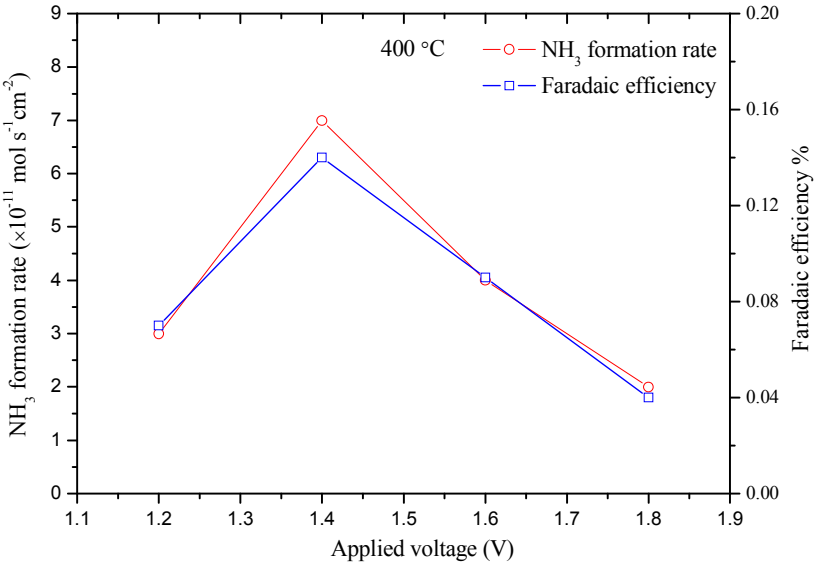

Fig. 9 Dependence of the rate of ammonia formation on the applied voltage at 400 °C